IDENTIFICATION OF MIXED OPERATIONAL MODES IN ROTORS SUBJECTED TO UNBALANCE FORCES: NUMERICAL AND EXPERIMENTAL METHODS

Alexandre Luiz Amarante Mesquita
Department of Mechanical Engineering, Federal University of Pará, UFPa, Belém, Brazil.
alexmesq@ufpa.br

Sérgio Junichi Idehara
Milton Dias Jr
Department of Mechanical Design, State University of Campinas, UNICAMP, Campinas, Brazil, P.O. Box 6122
milton@fem.unicamp.br

Abstract. *This paper discusses the existence of the mixed operational modes in flexible rotors subjected to unbalance forces. In this condition, some stations of the rotating machine describe their precessional movement in the forward direction while others move in the backward direction simultaneously. In the first part of the paper it is shown a method to identify the rotational speed range where occurs the mixed operational modes when there is an adjusted element finite model of the rotor. The method is based upon the Shape and Directivity Index (SDI) Plot. The value of SDI defines if a certain station (node) of a rotor is in forward or backward whirl. In the second part of the paper, it is shown an other method to identify the mixed modes. In this case, the methodology identifies the range of frequencies where occur the mixed operational modes, during an acceleration of the rotational speed of the rotating system. The method uses the directional order map, which is obtained through the application of the TVDFT order tracking technique in the complex response signal of the rotating system.*

Keywords*: vibration, rotordynamics, order tracking, operational modes.*

1. Introduction

It is well known that the unbalance force can excite the precessional backward modes only if the rotor is supported by bearings with different stiffness in two lateral orthogonal directions, as it happens in many rotors of rotating machinery (Vance, 1988; Ehrich, 1992; Krämer, 1993; Lalanne and Ferraris, 1997). Usually, bearings of rotating machines are designed to be anisotropic because it enhances the rotor stability. However, it may also introduce the undesirable unbalance-related backward whirling motion, which is known to cause reversal stress on the rotor, leading to premature failure of the system (Krämer, 1993). Fortunately, the rotational speed regions where the backward precession occurs are relatively narrow and close to the critical speeds, which are avoided as operational speeds. Among other things, the amount of damping on the rotor/bearings affects the existence, or not, of the backward precessional motion. Studies have shown that the more damping on the system, the narrower the rotational speed range where this motion can occur (Ehrich, 1992; Krämer, 1993).

The existence of the simultaneous forward and backward whirling on rotors has been proved experimentally by Rao *et al*. (1996,1997) and Muszynska (1996) but, in general, this phenomenon is briefly mentioned by the authors (Vance, 1988; Ehrich, 1992; Lee, 1993) and rarely discussed for flexible multi-discs rotors. Rao *et al* (1996,1997) studied a Jeffcott rotor supported on identical and dissimilar journal bearings. The authors showed the bearings clearance and the dissimilarities between the bearings affect the existence of the mixed operational modes. Muszynska (1996) studied a vertical, overhung unbalanced rotor with bent shaft and supported by anisotropic bearings and concluded that the combined effect of the mass unbalance together with the bow shaft unbalance could lead to simultaneous forward and backward precession motions at different stages of the rotor. Despite the fact that Lund (1974) presents many simulations in which this phenomenon can be observed, the author barely comments these results. Dias Jr. *et al*. (2002) and Miranda *et al*. (2002) showed experimentally the existence of the mixed operational modes in flexible rotors subjected to unbalance forces and the parameters that affect them.

The main goal of this work is to study, numerically and experimentally, the existence of the simultaneous forward and backward precessional motions on rotors subjected to unbalance forces. In the first part of the paper it is shown a method to identify the rotational speed range where occurs the mixed operational modes when there is an adjusted element finite model of the rotor. The method is based upon the Shape and Directivity Index (SDI) Plot, introduced by Dias and Allemang (2000). The value of SDI defines if a certain station (node) of a rotor is in forward or backward whirl. In the second part of the paper, it is shown an other method to identify the mixed modes. The methodology is based on experimental data and does not require a finite element model of the rotor. In this case, the technique identifies the range of frequencies where occur the mixed operational modes, during an acceleration of the rotational speed of the rotating system. The method uses the directional order map, which is obtained through the application of the TVDFT order tracking technique (Blough *et al*., 1996; Blough, 1998) in the complex response signal of the rotating system.

2. Unbalance Response – Complex Coordinates

It is well known that the use of complex coordinates on the study of rotating machines can help on the interpretation and visualization of the whirling modes. Thus, in this section, it is briefly presented the procedure for transforming the lateral, orthogonal displacement of each station of the rotor into their corresponding complex coordinates. It is also developed the frequency equation needed for the computation of the unbalanced response.

Let one first consider the well-known equation of motion of a 4N degrees of freedom rotating system with N stations (Ehrich, 1992):

$$[M]\{\ddot{q}\}+[D]\{\dot{q}\}+[K]\{q\}=\{Q\} \tag{1}$$

where $[M]$ is the symmetric, positive definite mass matrix. $[D]$ and $[K]$ are rotational speed dependent matrices and, in general, are not neither symmetric nor positive definite. Matrix $[D]$ represents the damping and gyroscopic terms and matrix $[K]$ includes the stiffness, circulatory, and internal damping, terms.

A very convenient way to assemble the displacement vector $\{q\}$ is the following:

$$\{q\}=\left\{\{y\}^T\{\phi_z\}^T\{z\}^T\{\phi_y\}^T\right\} \tag{2}$$

where $\{y\}$ and $\{z\}$ are the displacement vectors on each of the two directions perpendicular to the rotation axis of the rotor, and $\{\phi_y\}$ and $\{\phi_z\}$ are the angular displacement vectors of all stations (or nodes of a finite element model) in the directions *y* e *z*, respectively.

The expressions to transform the displacements of station *k* into their corresponding complex coordinates are:

$$p_{1k}=y_k(t)+jz_k(t) \quad \text{and} \quad p_{2k}=\phi_{zk}(t)-j\phi_{yk}(t)\ . \tag{3}$$

Considering all station (or nodes of the finite element model) one has:

$$\begin{Bmatrix}\{p\}\\ \{\bar{p}\}\end{Bmatrix}=\begin{Bmatrix}\{p_1\}\\ \{p_2\}\\ \{\bar{p}_1\}\\ \{\bar{p}_2\}\end{Bmatrix}=[T]^{-1}\begin{Bmatrix}\{y\}\\ \{\phi_z\}\\ \{z\}\\ \{\phi_y\}\end{Bmatrix}, \quad \text{where} \quad [T]=\frac{1}{2}\begin{bmatrix}[I] & [0] & [I] & [0]\\ [0] & [I] & [0] & [I]\\ -j[I] & [0] & j[I] & [0]\\ [0] & j[I] & [0] & -j[I]\end{bmatrix}, [T]^{-1}=\begin{bmatrix}[I] & [0] & j[I] & [0]\\ [0] & [I] & [0] & -j[I]\\ [I] & [0] & -j[I] & [0]\\ [0] & [I] & [0] & j[I]\end{bmatrix}. \tag{4}$$

Applying the same transformation $[T]$ on the force vector and substituting these results in Eq. (1) one obtains:

$$[M_C]\begin{Bmatrix}\{\ddot{p}\}\\ \{\ddot{\bar{p}}\}\end{Bmatrix}+[D_C]\begin{Bmatrix}\{\dot{p}\}\\ \{\dot{\bar{p}}\}\end{Bmatrix}+[K_C]\begin{Bmatrix}\{p\}\\ \{\bar{p}\}\end{Bmatrix}=\begin{Bmatrix}\{g\}\\ \{\bar{g}\}\end{Bmatrix}, \tag{5}$$

where $[M_c]$, $[D_c]$ and $[K_c]$ are the complex mass, complex damping/gyroscopic, and complex stiffness/circulatory matrices. $\{g\}$ is the complex force vector.

The complex displacement $\{p\}$ as well as the complex external force $\{g\}$ can be decomposed into their forward, $\{P_f\}$ and $\{G_f\}$, and backward, $\{P_b\}$ and $\{G_b\}$, components as:

$$\{p(t)\}=\{P_f\}e^{j\omega t}+\{P_b\}e^{-j\omega t} \quad \text{and} \quad \{g(t)\}=\{G_f\}e^{j\omega t}+\{G_b\}e^{-j\omega t}\ . \tag{6}$$

Substituting Eq.(6) in Eq.(5) one concludes that

$$(-\omega^2[M_C]+j\omega[D_C]+[K_C])\begin{Bmatrix}\{P_f\}\\ \{\bar{P}_b\}\end{Bmatrix}=\begin{Bmatrix}\{G_f\}\\ \{\bar{G}_b\}\end{Bmatrix} \tag{7}$$

It is known the unbalance force is pure forward and its amplitude vector $\{G_f\}$ is a function of the unbalance $m\varepsilon$ and of the initial phase of the unbalance mass, and of the rotational speed of the rotor. The backward component of the unbalance force is zero. Therefore, the steady state unbalance response of the rotating system is obtained trough the solution of the following set of algebraic equations:

$$(-\Omega^2[M_C]+ j\Omega[D_C]+[K_C])\begin{Bmatrix}\{P_f\}\\ \{\bar{P}_b\}\end{Bmatrix}=\begin{Bmatrix}\{G_f\}\\ \{0\}\end{Bmatrix} \tag{8}$$

The relative amplitude between the forward, $\{P_f\}$, and the backward, $\{P_b\}$, components of the unbalance response define whether the precessional motion of a specific station of the rotor will be forward (when $P_f > P_b$) or backward (when $P_f < P_b$). If some stations of the rotor describe their precessional movements in the forward direction while others move in the backward direction simultaneously, then it is characterized the occurrence of a mixed operational mode. These two components can be combined in one parameter, called Shape and Directivity Index, or SDI, defined by Han and Lee (1999), that define whether the precessional motion of a specific station of the rotor will be forward or backward, circular, elliptical or rectilinear, i. e.:

$$-1 \le SDI = \frac{|P_f| - |P_b|}{|P_f| + |P_b|} \le 1 \tag{9}$$

The relations among the values of the SDI, the shape of the orbit of a station of the rotor and the direction of the precessional motion are:

- SDI = -1 ⇒ Circular backward precessional motion
- -1 < SDI < 0 ⇒ Elliptical backward precessional motion
- SDI = 0 ⇒ Rectilinear motion
- 0 < SDI < 1 ⇒ Elliptical forward precessional motion
- SDI = 1 ⇒ Circular forward precessional motion

It is easy to conclude that the sign of the SDI defines the direction of the precessional motion while the shape of the orbit is defined by its absolute value. A very convenient way to visualize how each station of the rotor whirls when it is subjected to unbalance forces is through the *SDI Plot*. This plot is built by computing the SDI for all nodes and each rotational speed. Specific colors are assigned to each SDI value and a convenient color map must be used in order to be possible to easily distinguish between backward and forward precessional motion of the stations of the rotor. Figure 1 shows an example of a SDI Plot for a single rotor.

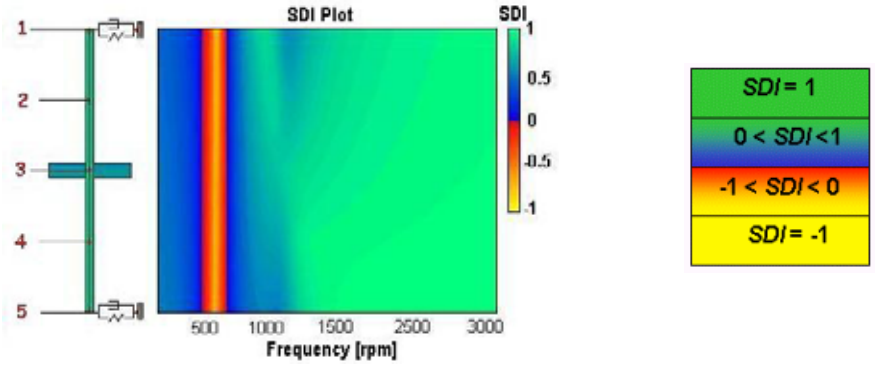

Figure 1. SDI Plot for a single rotor.

3. Numerical Results

In order to investigate the existence of the mixed operational modes, a flexible rotor with three discs and two bearings is studied (Lallane and Ferraris, 1997, pg. 126). Figure 2 shows the finite element model of the rotor. The localization of discs is listed in Table 1. Shaft and discs are made of steel and the dimensions of the discs are listed in Table 2. The bearings are modeled with the following parameters: $k_{yy}=7\times10^7$N/m, $k_{zz}=5\times10^7$N/m, $c_{yy}=7\times10^2$ Ns/m, $c_{zz}=5\times10^2$ Ns/m, $k_{yz}=k_{zy}=c_{yz}=c_{zy}=0$. According Fig. 2 and Fig. 3, all stations move in forward precession from 0 (zero) to 344 rpm. Between 344 rpm and 3572 rpm, the band where is located the first critical speed (3490 rpm), all stations are moving in backward direction. After 3572 rpm all station move in forward direction again until close to 8000rpm. There is a range of frequencies between around 8000 and 9100 rpm where mixed mode occurs. In this range of frequencies, the nodes 1 to 11 move in backward direction while the nodes 12 to 27 move in forward whirl. Figure 4 shows an operational mode for a rotational speed of 9004.8 rpm and the values of SDI for the nodes of the rotating system in this operational mode.

Table 1: Distances in between discs and bearings.

A-D1	0.2 m
D1-D2	0.3 m
D2-D3	0.5 m
D3-B	0.3 m

Table 2: Disc data.

Disc	D1	D2	D3
Thickness [m]	0.05	0.05	0.06
Inner radius [m]	0.05	0.05	0.05
Outer radius [m]	0.12	0.2	0.2

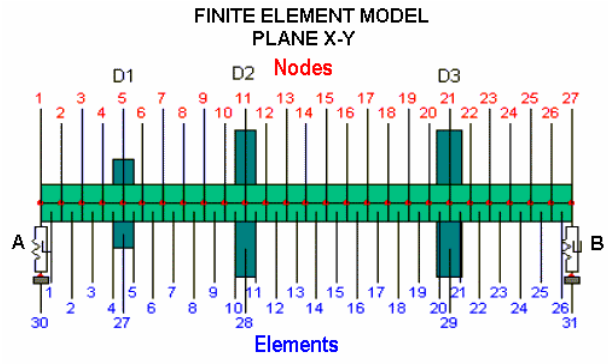

Figure2: Finite Element Model of the rotor.

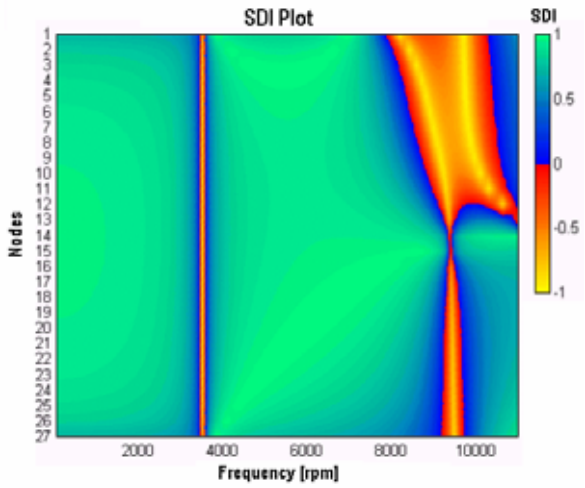

Figure 3: SDI Plot for the rotor.

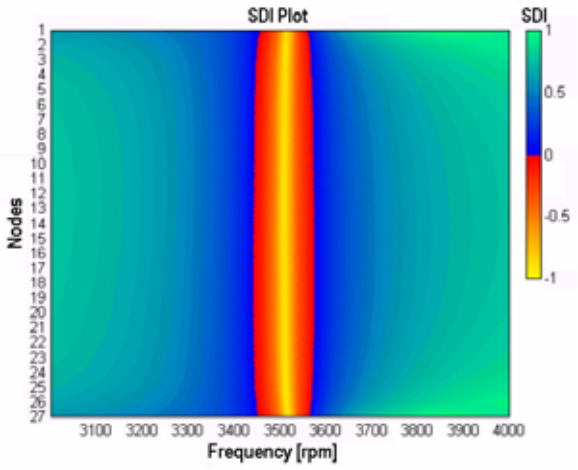

Figure 4: Zoom in the SDI Plot for the rotor.

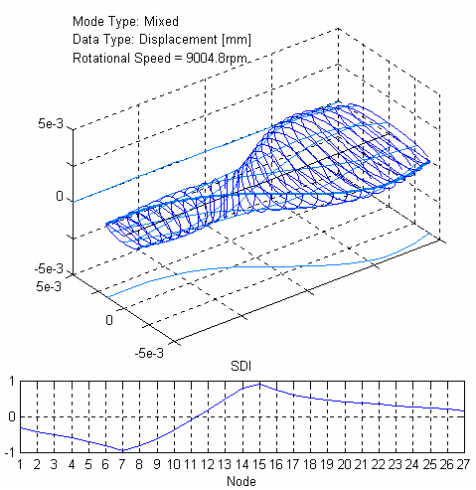

Figure 5: Mixed Operational Mode for 9004.8 rpm.

Therefore, when there is an adjusted model of a rotor, the SDI Plot is able to identify the frequencies where mixed operational mode occurs. Without a model of the rotor it becomes difficult to identify such a range of frequencies. In the next section it is shown a methodology for this case. The method identifies the range of frequencies where occur the mixed operational modes during an acceleration of the rotational speed of the rotating system. The method uses the directional order map, which is obtained trough the application of the TVDFT order tracking technique in the complex response signal of the rotating system.

4. Order Tracking Techniques

The order tracking analysis is a measurement technique suitable for variable speed machines. Most of the order tracking methods require sampling of the vibration signal at constant angle increments and hence at a sampling rate proportional to the shaft speed of the machine (Fyfe and Munck, 1997; Blough, 1998). As a result, in a waterfall plot, the frequency spectrum components can be displayed as stationary lines versus orders (multiples of the shaft rotation) instead of frequency, in Hz. Order tracking techniques identify the orders amplitudes and phases in variable speed machines. There are different methods of order tracking, such as, the Computed Order Tracking (COT) (Potter, 1990),

the Digital Resampling (Blough, 1998) and the TVDFT (Time Variant Discrete Fourier Transform) (Blough *et al*., 1996; Blough, 1998).

The COT and Digital Resampling methods can be classified as digital resampling based order tracking, and they are the most common order tracking methods in use in commercial softwares and dynamic signal analyzers (Blough, 1998). Recently, some new methods of order tracking have been developed such as the Kalman filter based methods (Vold *et al*., 1993, 1997) and the TVDFT method. The former will not be treated in this paper. The Time Variant Discrete Fourier Transform (TVDFT) is an order tracking method but does not resample the vibration data. It is performed directly on data that is sampled with a constant time interval, reducing considerably the computational effort. As any order tracking method, the TVDFT is also very sensitive to the quality of the instantaneous frequency measurement, i.e., its accuracy depends on the quality of the tachometer signal processing.

The TVDFT is a special case of the chirp-z transform. The chirp-z transform is defined as a type of Fourier transform with a kernel whose frequency and damping vary as a function of time. The TVDFT is defined as a discrete Fourier transform whose kernel frequency varies as a function of time defined by the rpm of the machine, but the damping does not vary as a function of time. This kernel is a cosine or sine function of unitary amplitude and an instantaneous frequency equal to that of the tracked order at each instant of time. Its expressions are presented in Eq.(10a) and Eq.(10b):

$$a_m = \frac{1}{N}\sum_{n=1}^{N} x(n.\Delta t)\cos\left(2\pi\int_0^{n.\Delta t}(O_m.\Delta t.\frac{rpm}{60})dt\right) \tag{10a}$$

$$b_m = \frac{1}{N}\sum_{n=1}^{N} x(n.\Delta t)\,sen\left(2\pi\int_0^{n.\Delta t}(O_m.\Delta t.\frac{rpm}{60})dt\right), \tag{10b}$$

where O_m is the order which is being analyzed, x is the operating data, N is the block size of the transform, Δt is the sampling interval, a_m is the Fourier coefficient of the cosine term for O_m, b_m is the Fourier coefficient of the sine term for O_m, and rpm is the instantaneous rpm of the machine.

In order to obtain better results when orders are either very close together or crossing one another, an orthogonality compensation matrix (OCM) may be applied. The application of the OCM also allows faster sweep rates to be analyzed more accurately. The OCM may be applied in a post-processing step to the order estimates from a TVDFT analysis. Very close orders are normally difficult to be separated using resampling techniques, as well as in the TVDFT. Nevertheless, if the OCM is used, these close orders can be separated effectively (Blough, 1998). The formulation of OCM is a set of linear equations formulations that must be solved for each rpm value:

$$\begin{bmatrix} e_{11} & e_{12} & e_{13} & \cdots & e_{1m} \\ e_{21} & e_{22} & e_{23} & & e_{2m} \\ e_{31} & e_{32} & e_{33} & & e_{3m} \\ \vdots & & & & \vdots \\ e_{m1} & & \cdots & & e_{mm} \end{bmatrix} \begin{Bmatrix} o_1 \\ o_2 \\ o_3 \\ \vdots \\ o_m \end{Bmatrix} = \begin{Bmatrix} \tilde{o}_1 \\ \tilde{o}_2 \\ \tilde{o}_3 \\ \vdots \\ \tilde{o}_m \end{Bmatrix}. \tag{11}$$

where e_{ij} is the cross orthogonality contribution of order i in the estimate of order j, O_i is the compensated value of order i, and $\tilde{O}_i$ is the estimated value of order i obtained using the TVDFT. The terms, e_{ij}, are calculated as follow:

$$e_{ij} = \frac{1}{N}\sum_{n=1}^{N}\left\{\exp\left(2\pi\int_0^{n.\Delta t}(o_i.\Delta t.\frac{Rpm}{60})dt\right).\times(window)\exp\left(2\pi\int_0^{n.\Delta t}(o_j.\Delta t.\frac{Rpm}{60})dt\right)\right\} \tag{12}$$

Equation (11) is solved by multiplying both sides by the inverse of OCM. The resulting order estimates are linearly independent to one another.

5. Experimental Results

The experimental part of this work was performed using the test rig pictured in Fig. 6. This experimental set up consists of a Bently rotor kit assembly powered by 1 HP electric motor. There are two rigid discs mounted on a shaft supported by two bearings. The bearing closer to the motor is named bearing I and the other is the bearing II. The anisotropic bearing II is supported by different sets of springs in horizontal and vertical directions (to provide forward and backward whirl) (Fig. 7). There are 8 displacement sensors to measure data from 4 different stations: the two discs

and two stations in the shaft. A National Instrument data acquisition board, controlled by a Matlab® code was used to acquire the unbalance responses of the rotating system.

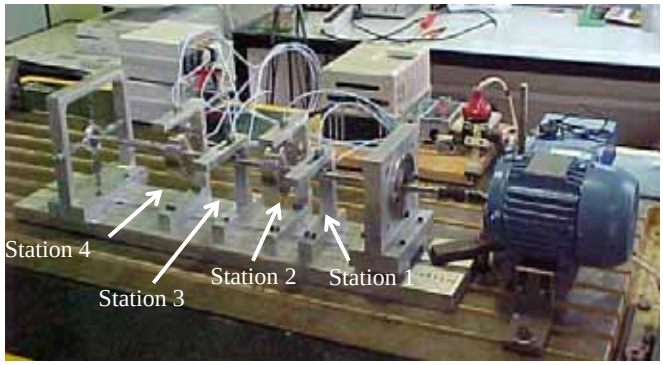

Figure 6. Test rig used in the analysis.

Figure 7. Anisotropically supported rolling bearing.

It was used a band pass filter to ensure that only the frequency component relative to the rotor unbalance response were present in the analysis. The run-up was measured from 52 Hz to 58 Hz in 10 seconds. After the application of the TVDFT order tracking in the complex and nonstationary data $p(t)$, the resultant order map is obtained. This order map shows that all stations move in forward direction. Figure 8 presents the directional order map for station 1, and also shows the magnitude of P_f and P_b as function of time and rotation.

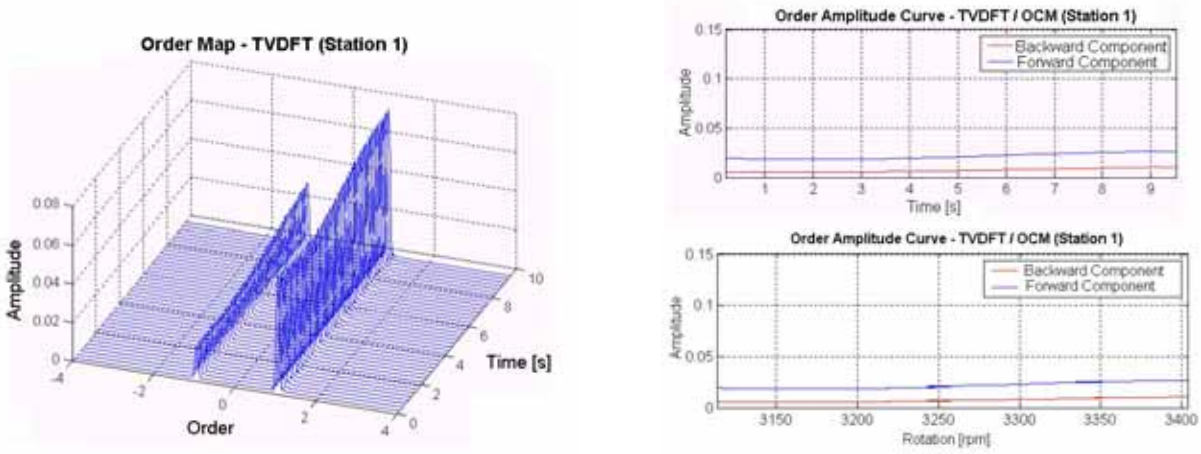

Figure 8. Directional order map for station 1 and magnitude of P_f and P_b as function of time and rotation.

Another test was performed, but with the disc II (disc closer to the anisotropic bearing II) rotated by 90° in comparison with another disc. It means there was a new spatial distribution of unbalance forces in the system. As a result, the stations 1, 2 and 4 move in forward direction in all range of frequency, while for the station 3 there is a change in the whirl direction. The precessional movement of this station is in forward direction until 3275 rpm. After that, the station moves in backward direction. This changing in whirl direction can be visualized in Fig. 9. Thus, in this case, in the range of 3275 rpm until 3518 rpm, the rotating system has mixed operational modes.

In a third analysis, another 90° rotation in disc II was made. As a result, the stations 1 and 2 still move in forward direction, but the stations 3 and 4 now move in backward direction during the range of frequency used. This situation means that there are mixed modes over all these frequencies. Fig. 10 shows the order map and the order amplitude curve for station 1, and Fig. 11 shows the order map and the order amplitude curve for station 3.

The experimental results confirmed that the occurrence of the mixed operational modes phenomenon is strongly affected by the spatial unbalance force distribution, as has been pointed out in the works of Dias Jr. *et al*. (2002). The different distribution of unbalance forces in the system was achieved by changing the relative angular position of the unbalance masses of the discs (through the rotation of the disc II in comparison to disc I).

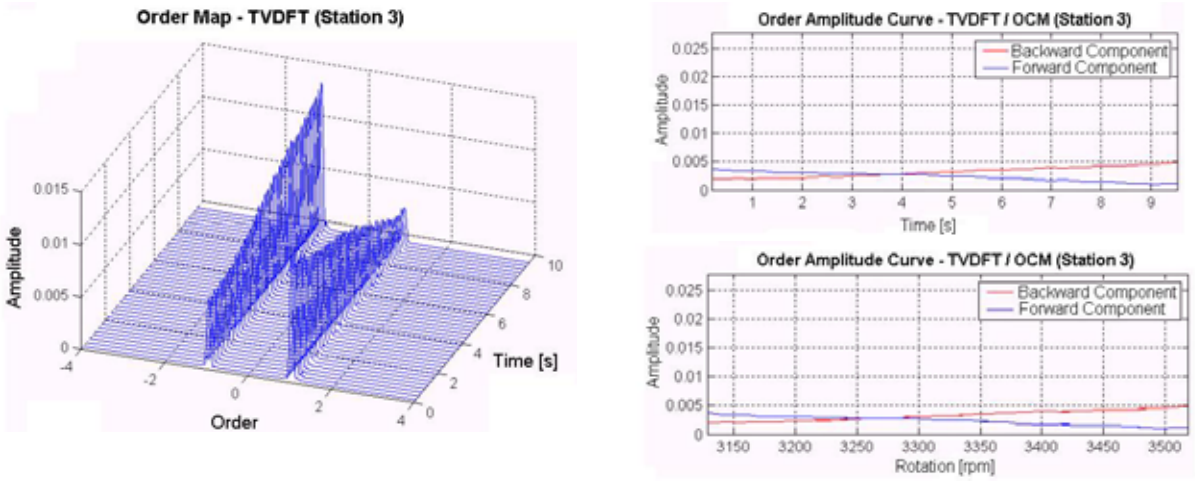

Figure 9. Directional order map for station 3 and magnitude of P_f and P_b as function of time and rotation. Disc II rotated by 90°.

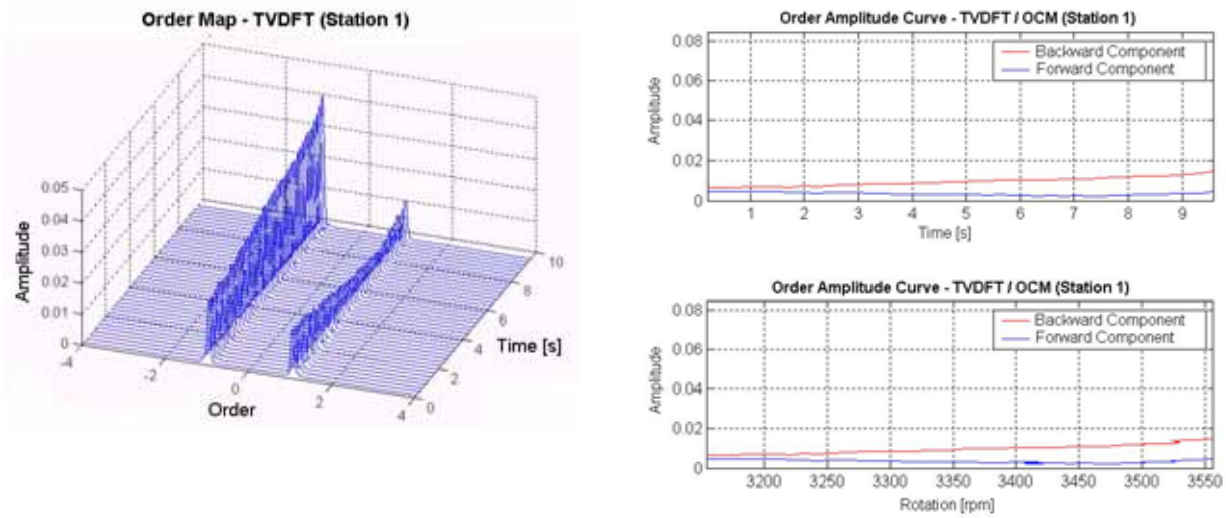

Figure 10. Directional order map for station 1 and magnitude of P_f and P_b as function of time and rotation. Disc II rotated by 180°.

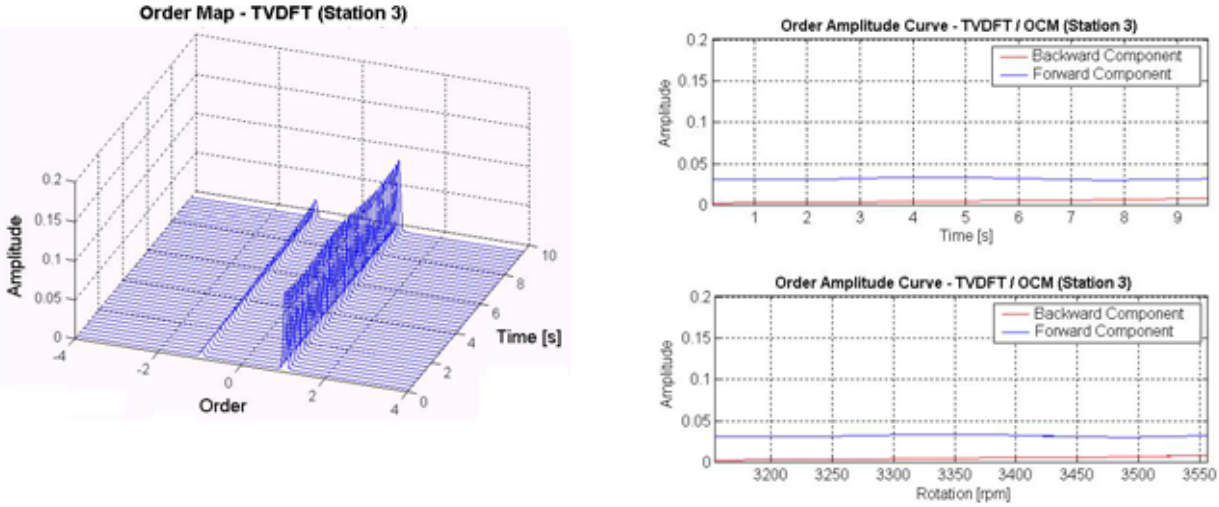

Figure 11. Directional order map for station 3 and magnitude of P_f and P_b as function of time and rotation. Disc II rotated by 180°.

6. Concluding Remarks

In the first part of the paper it is shown a method to identify the rotational speed range where occurs the mixed operational modes when there is an adjusted element finite model of the rotor. The method is based upon the Shape and Directivity Index (SDI) Plot. The value of SDI defines if a certain station (node) of a rotor is in forward or backward whirl. The second part of the paper, it is presented a methodology to identify the range of frequencies where occur the mixed operational modes, during an acceleration of the rotational speed of the rotating system. The method uses the directional order map, which is obtained trough the application of the TVDFT order tracking technique in the complex response signal of the rotating system

The experimental method is applied in test rig, which consist of two rigid discs mounted on a shaft supported by one rigid and one anisotropic rolling bearing at the ends. The experimental data confirmed the existence of the mixed operational modes in the system. The results demonstrated that this phenomenon is strongly affected by the spatial unbalance distribution (relative angular position and amount of the unbalance masses). This methodology has as disadvantages the need of a high sample rate in the signals, in order to have a good measurement of the tachometer signal and consequently a good estimation of the instantaneous rotational speed. Due this high sample rate it is necessary more computational effort to perform the proposed analysis.

7. Acknowledgements

The authors would like to thank to CAPES (Coordenação de Aperfeiçoamento de Pessoal ne Nível Superior) and CNPq (Conselho Nacional de Pesquisa e Desenvolvimento) for financial support of this project.

8. References

Blough, J. R., 1998, “Improving the Analysis of Operating Data on Rotating Automotive Components”, Department of Mechanical, Industrial, and Nuclear Engineering of the College of Engineering, University of Cincinnati, Cincinnati.

Blough, J. R., Brown D. L. and Vold, H., 1996, “Order Tracking With Time Variant Discrete Fourier Transform”, Proceedings of the 21st International Seminar of Modal Analysis - Noise and Vibration Engineering, Leuven, Belgium, pp. 1515-1525.

Dias Jr., M. and Allemang, R.J., 2000, “Some Insights into the Simultaneous Forward and Backward Whirling of Rotors”, XX International Modal Analysis Conference.

Dias Jr., M., Idehara, S.J., Mesquita, A.L.A. and Miranda, U.A., 2002, “On the Simultaneous Forward and Backward Whirling of Flexible Rotors: Numerical Analysis and Experimental Verification”, IFToMM, 6th International Conference on Rotor Dynamics, Sydney, Australia, pp. 496-503.

Ehrich, F.F. (editor), 1992, “Handbook of Rotordynamic”, New York: McGraw-Hill Inc.

Fyfe, K. and Munck, D., 1997, “Analysis of Computed Order Tracking”, Mechanical System and Signal Processing, Vol. 11, No.2, pp. 187 - 205.

Han, Y.S., Lee, C.W., 1999, “Directional Wigner Distribution for Order Analysis in Rotating/Reciprocating Machines”. Mechanical System and Signal Processing, Vol.13, No.5, pp. 723-737.

Krämer, E., 1993, “Dynamics of Rotors and Foundations”, Berlin: Springer-Verlag.

Lalanne, M. and Ferraris, G., 1998, “Rotordynamics Predictions in Engineering”, 2nd edition. John Wiley & Sons.

Lee, C.W., 1993, “Vibration Analysis of Rotors”, Kluwer Academic Publishers.

Lund, J.W., 1974, “Modal Response of a Flexible Rotor in Fluid-Film Bearing”, Transactions of ASME - Journal of Engineering for Industry, pp 525-532.

Miranda, U.A., Dias Jr., M., Mesquita, A.L.A. and Idehara, S.J., 2002, “On the Application of Directional Time-Frequency Distribution to the Identification of Simultaneous Forward and Backward Whirling in Flexible Rotors”, IFToMM, 6th International Conference on Rotor Dynamics, Sydney, Australia, pp. 504-511.

Muszynska, A., 1996, “Forward and Backward Precession of a Vertical Anisotropically Supported Rotor”, Journal of Sound and Vibration, Vol.192, No. 1, pp 207-222.

Potter, R., 1990, “A New Order Tracking Method for Rotating Machinery”. Sound and Vibration Magazine, Vol.24, No.9, pp.30-34.

Rao, C., Bhat, R. and Xistris, G.D., 1996, “Experimental Verification of Simultaneous Forward and Backward Whirling at Different Points of a Jeffcott Rotor Supported on Identical Journal Bearings”, Journal of Sound and Vibration, Vol.128, No.3, pp 379-388.

Rao, C., Bhat, R. and Xistris, G.D., 1996, “Simultaneous Forward and Backward Whirling in a Jeffcott Rotor Supported on Dissimilar Hydrodinamic Bearing”, Journal of Sound and Vibration, Vol. 203, No.4, pp 707-716.

Vance J.M., 1988, “Rotordynamics of Turbomachinery”, John Wiley & Sons.

Vold, H. and Leuridan, J., 1993, “High Resolution Order Tracking At Extreme Slew Rates, Using Kalman Tracking Filters”, Proceedings of the Noise and Vibration Conference, SAE Technical Paper 931288, Tranverse City, MI, USA.

Vold, H., Mains, M. and Blough, J. R., 1997, “Theoretical Foundations For High Performance Order Tracking With The Vold-Kalman Filter”. Proceedings of the Noise and Vibration Conference, SAE Technical Paper 972007, Traverse City, MI, USA.